Stem Cell Reports
Article

OPEN ACCESS

FGF10-FGFR2B Signaling Generates Basal Cells and Drives Alveolar Epithelial Regeneration by Bronchial Epithelial Stem Cells after Lung Injury

Tingting Yuan,[1,8] Thomas Volckaert,[1,8] Elizabeth F. Redente,[2,3] Seantel Hopkins,[1] Kylie Klinkhammer,[1] Roxana Wasnick,[4] Cho-Ming Chao,[4] Jie Yuan,[1] Jin-San Zhang,[5] Changfu Yao,[6] Susan Majka,[7] Barry R. Stripp,[6] Andreas Günther,[4] David W.H. Riches,[2,3] Saverio Bellusci,[4] Victor J. Thannickal,[1] and Stijn P. De Langhe[1,*]

[1]Department of Medicine, Division of Pulmonary, Allergy & Critical Care Medicine, University of Alabama at Birmingham, THT 422, 1720 2nd Avenue S., Birmingham, 35294-2182 AL, USA
[2]Department of Pediatrics, Division of Cell Biology, National Jewish Health, Denver, CO 80206, USA
[3]Denver Veteran Affairs Medical Center, Denver, CO 80206, USA
[4]German Center for Lung Research, Excellence Cluster Cardio-Pulmonary System, Universities of Giessen and Marburg Lung Center, 35392 Giessen, Germany
[5]School of Pharmaceutical Sciences, First Affiliated Hospital, Wenzhou Medical University, Wenzhou, Zhejiang 325035, China
[6]Women's Guild Lung Institute, Department of Medicine, Cedars-Sinai Medical Center, Los Angeles, CA 90048, USA
[7]Department of Medicine, National Jewish Health, Denver, CO 80206, USA
[8]Co-first author
*Correspondence: sdelanghe@uabmc.edu
https://doi.org/10.1016/j.stemcr.2019.04.003

SUMMARY

Idiopathic pulmonary fibrosis is a common form of interstitial lung disease resulting in alveolar remodeling and progressive loss of pulmonary function because of chronic alveolar injury and failure to regenerate the respiratory epithelium. Histologically, fibrotic lesions and honeycomb structures expressing atypical proximal airway epithelial markers replace alveolar structures, the latter normally lined by alveolar type 1 (AT1) and AT2 cells. Bronchial epithelial stem cells (BESCs) can give rise to AT2 and AT1 cells or honeycomb cysts following bleomycin-mediated lung injury. However, little is known about what controls this binary decision or whether this decision can be reversed. Here we report that inactivation of *Fgfr2b* in BESCs impairs their contribution to both alveolar epithelial regeneration and honeycomb cysts after bleomycin injury. By contrast overexpression of *Fgf10* in BESCs enhances fibrosis resolution by favoring the more desirable outcome of alveolar epithelial regeneration over the development of pathologic honeycomb cysts.

INTRODUCTION

Idiopathic pulmonary fibrosis (IPF) is a common form of interstitial lung disease resulting in alveolar remodeling and progressive loss of pulmonary function, respiratory failure, and death, often within 5 years of diagnosis (King et al., 2011; Steele and Schwartz, 2013). IPF pathogenesis encompasses fibrotic remodeling, inflammation, and loss of lung architecture (Barkauskas and Noble, 2014). Although the underlying causes of IPF remain elusive, genetic, and experimental evidence support the concept that chronic alveolar injury and failure to properly repair the respiratory epithelium represent key pathogenic mechanisms (Camelo et al., 2014; Thannickal et al., 2004; Yang et al., 2013). Histologically, respiratory epithelial cells of the lung parenchyma express atypical proximal airway epithelial and indeterminate cell-type markers (Plantier et al., 2011; Seibold et al., 2013), including goblet and basal cell (BC) characteristics that are normally restricted to conducting airways. Fibrotic lesions and bronchiolized or honeycomb structures replace alveolar structures, the latter normally lined by alveolar type 1 (AT1) and AT2 cells. Genome-wide transcriptome analyses of lung tissue and isolated epithelial cells from IPF patients demonstrate dramatic changes in ciliated, basal, and goblet cell-associated gene expression and loss of normal alveolar epithelial cells, reflecting profound changes in epithelial cell differentiation and function in IPF (Kropski et al., 2015; Seibold et al., 2013; Xu et al., 2016).

It is now generally accepted that insults to the alveolar epithelium, resulting in a loss of AT2 stem cells or mutations in alveolar epithelial cells that either impair their self-renewal and/or impair their differentiation into AT1 cells, can serve as a trigger of pulmonary fibrosis (Barkauskas and Noble, 2014). However, functional abnormalities in bronchiolar epithelial cells (and not just alveolar epithelial cells) can predispose patients to development of IPF. A gain-of-function mutation in mucin 5B (*MUC5B*), which is specifically expressed by club, mucous, and goblet cells (Evans et al., 2004; Ostedgaard et al., 2017; Roy et al., 2011, 2014), and which results in a 30-fold increase in *MUC5B* expression, is associated with increased risk of both familial and sporadic IPF (Seibold et al., 2011; Zhang et al., 2011). Overexpression of *Muc5b* also causes mucociliary dysfunction and enhances lung fibrosis in mice (Hancock et al., 2018). The precise mechanism by which this genetic variant leads to fibrosis is unknown, but one possibility is that trapped harmful agents cause damage to this stem cell population and therefore affect bronchial epithelial-mediated alveolar epithelial regeneration (Li et al., 2012; Roy et al., 2014).

Several studies have shown that subsets of SCGB1A1$^+$ bronchial epithelial club cells can give rise to AT1 and AT2 cells following bleomycin-mediated lung injury, yet these findings remain somewhat controversial in the field largely because of the reliance on single CreER(T2) lines (Barkauskas et al., 2013; Guha et al., 2017; Kim et al., 2005; Kumar et al., 2011; Lee et al., 2014; McQualter et al., 2010; Rock et al., 2011; Zheng et al., 2012, 2013). In the mouse bleomycin model, ~50% of new AT2 cells which appear after bleomycin injury are thought to be derived from subsets of bronchial epithelial cells, whereas ~40% are thought to be derived from pre-existing AT2 cells (Barkauskas et al., 2013). However, the contribution of each stem cell population largely depends on the severity of the injury. *p63*$^+$*/Scgb1a1*$^+$*/Sox2*$^+$ bronchial epithelial stem cell (BESCs) have been shown to invade the lung parenchyma after severe influenza-mediated lung injury and give rise to neo-BCs in response to HIF1α-mediated Notch signaling, or AT2 cells in response to increased β-catenin signaling (Kumar et al., 2011; Ray et al., 2016; Vaughan et al., 2015; Xi et al., 2017; Yang et al., 2018; Zuo et al., 2015). Whether these cells respond in a similar fashion to other types of injury such as bleomycin injury has not yet been investigated. BESCs are thought to be a reserve stem cell population that helps in regeneration of the alveolar epithelium when most AT2 stem cells have been exhausted. However, in IPF it appears that this backup repair mechanism is severely impaired, resulting instead in the development of bronchiolized regions in the lung parenchyma lined with BCs that are referred to as "honeycomb cysts."

We have previously shown that FGFR2B signaling is required for tracheal BC maintenance and that *Fgf10* overexpression can induce p63 (BC marker) and SFTPC (AT2 cell marker) expression in club cells (Balasooriya et al., 2017; Volckaert et al., 2013, 2017). Importantly, FGF10 levels are reduced in lungs from aged mice before and after injury as well as in IPF subjects with progressive compared with stable disease (Chanda et al., 2016). In addition, we previously demonstrated that *Fgf10*-expressing lipofibroblasts (LIFs), which form the AT2 stem cell niche, differentiate into myofibroblasts upon bleomycin injury (El Agha et al., 2017). In the present study, we demonstrate that FGF10-FGFR2B signaling also actively maintains AT2 stem cells. We now demonstrate, using single-cell RNA sequencing (RNA-seq), that these *Fgf10*-expressing fibroblasts downregulate *Fgf10* expression upon injury. Furthermore, we show that loss of FGF10-FGFR2B signaling in bronchial epithelial cells impairs the generation of both neo-BCs and alveolar epithelial (AT1 and AT2) cells after bleomycin injury. By contrast, *Fgf10* overexpression in bronchial epithelial cells promotes their differentiation along the AT2 lineage rather than the BC lineage after injury. Taken together, our findings suggest that reduced levels of *Fgf10* compromise alveolar epithelial regeneration by BESCs and we demonstrate that exogenous FGF10 can promote the differentiation of BESCs along more desirable reparative alveolar epithelial lineages.

RESULTS

FGF10-FGFR2B Signaling Is Required for Maintaining AT2 Cells

We have recently shown that FGF10-FGFR2B signaling drives BC development and is also required for adult BC maintenance (Volckaert et al., 2013, 2017). However, BCs are not the only stem cell population that depends on an *Fgf10*-expressing niche in the adult lung. In the adult lung, every AT2 cell sits adjacent to an *Fgf10*-expressing LIF, which forms the AT2 stem cell niche (Figures 1A and 1B). However, these *Fgf10*-expressing AT2 niche cells differentiate into myofibroblasts upon bleomycin injury (Figures 1C and 1D) (El Agha et al., 2017). Interestingly, while lung FGF10 levels increase after bleomycin injury, it is unclear whether this increase is caused by an increase in the number of *Fgf10*-expressing fibroblasts or whether individual fibroblasts express more *Fgf10*. To investigate this question, we reanalyzed single-cell RNA-seq data on isolated EPCAM$^-$CD31$^-$CD45$^-$ stromal cells from uninjured or injured *αSMA-GFP;Tbx4-Cre;Rosa26-tdTomato* lungs 3 weeks after bleomycin treatment (Xie et al., 2018). We found that individual *Fgf10*-expressing stromal cells expressed lower levels of *Fgf10* in injured compared with uninjured lungs (Figure 1E), but that the total number of *Fgf10*-expressing fibroblasts increased after injury. Interestingly, haploinsufficiency for *FGF10* has been linked to the development of emphysema in humans (Klar et al., 2011) suggesting that tonic FGF10 signaling may not only be required for BCs but also for AT2 cell maintenance. As each AT2 cell is closely juxtaposed to an *Fgf10*-expressing LIF (Figures 1A and 1B), we hypothesized that AT2 stem cells require high local levels of FGF10 for their maintenance.

To investigate this we inactivated the FGF10 receptor, *Fgfr2b*, in mature AT2 cells of adult *Sftpc*^{CreERT2}*;Fgfr2b*$^{f/f}$*; mTmG* mice and found that this resulted in a nearly complete loss of AT2 cells (Figure 1F) and have a reduced capacity to regenerate alveolar epithelium after bleomycin injury (Figure 1G) (note that Cre activity before and after tamoxifen treatment of all the different mouse lines used in this manuscript is documented in Figures S1 and S2). In conclusion, our data demonstrate that FGFR2B signaling is required to actively maintain AT2 and BCs during adult life.

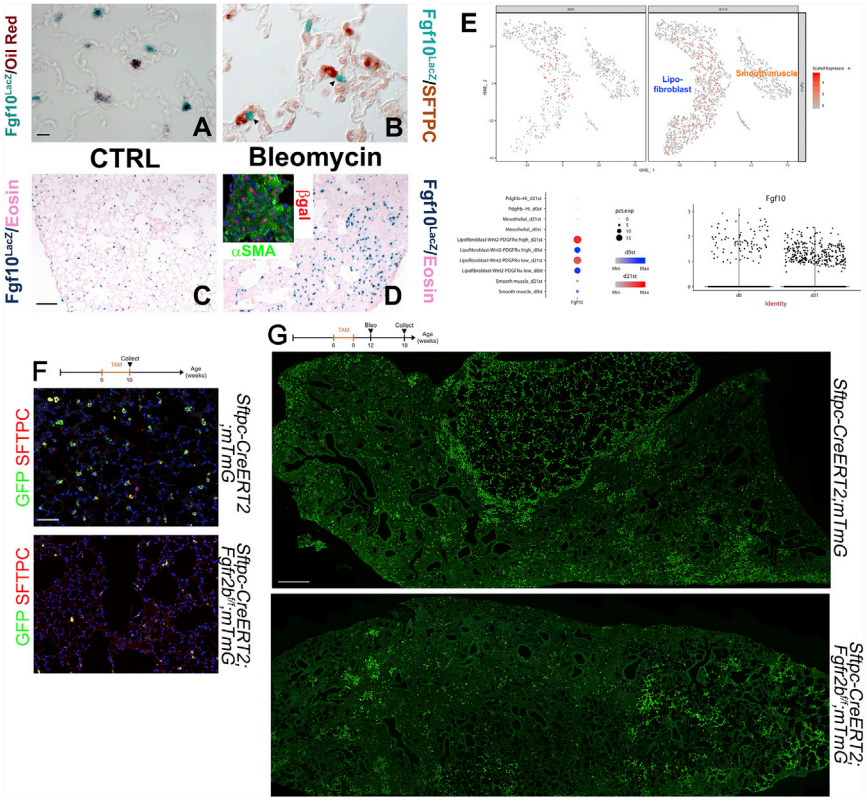

Figure 1. Fgf10-Fgfr2b Signaling Is Required for AT2 Stem Cell Maintenance

(A) β-Gal (blue) and oil red (LIF marker) staining on frozen sections of 3-month-old *Fgf10*^{LacZ} lungs shows that LIFs express *Fgf10*.

(B) β-Gal (blue) and immunostaining for SFTPC (brown) on paraffin sections of 3-month-old *Fgf10*^{LacZ} lungs shows LIFs located adjacent to AT2 cells.

(C and D) β-Gal and eosin staining on *Fgf10*^{LacZ} lungs 21 days after saline (C) and bleomycin treatment (D). Inset in (D) shows coimmunostaining for α-SMA (MYF marker) and β-gal (FGF10), demonstrating that LIFs transdifferentiate into MYFs after bleomycin injury.

(E) Single-cell RNA-seq analysis on GFP^{+}, EPCAM^{-}, CD45^{-}, TER119^{-} sorted fibroblasts isolated from *Tbx4*^{CreERT2};*mTmG* mice show fewer LIFs expressing higher levels of *Fgf10* in noninjured lungs compared with lungs 3 weeks after bleomycin injury.

(F) Immunostaining for GFP and SFTPC (AT2 cell) on *Sftpc*^{CreERT2};*mTmG* and *Sftpc*^{CreERT2};*Fgfr2b*$^{f/f}$;*mTmG* lungs 4 weeks after being placed on tamoxifen chow.

(G) Immunostaining for GFP (AT2 cell and descendant) on *Sftpc*^{CreERT2};*mTmG* and *Sftpc*^{CreERT2};*Fgfr2b*$^{f/f}$;*mTmG* lungs 6 weeks after bleomycin treatment.

Scale bars, 10 μm (A), 100 μm (C), 50 μm, and (F) 500 μm (G).

FGF10-FGFR2B Signaling in Bronchial Epithelium Generates Neo-Basal and Alveolar Epithelial Cells after Bleomycin Injury

We recently reported that overexpression of *Fgf10* is sufficient to induce the expression of basal and AT2 cell markers in club cells (Volckaert et al., 2017). The dependence of both BCs and AT2 cells on FGF10-FGFR2B signaling raises the question of whether different levels of FGF10-FGFR2B signaling in bronchial epithelial cells may be required for alveolar epithelial regeneration versus BC expansion that leads to distal bronchiolization and generation of honeycomb cysts after bleomycin injury. To investigate this, we inactivated *Fgfr2b* in all bronchial epithelial cells using *Sox2*^{CreERT2};*Fgfr2b*$^{f/f}$ mice or in club cells specifically using *Scgb1a1*^{CreERT2};*Fgfr2b*$^{f/f}$ mice while simultaneously lineage tracing them with an mTmG or Confetti reporter. Our data suggest that both alveolar epithelial regeneration and the generation of neo-BCs at sites of injury is impaired in these mice (Figures 2A, 2C–2L, and S3A–S3E). This incapacity of BESCs to invade the lung parenchyma after bleomycin injury resulted in large holes near the BADJ of injured mutant lungs (Figure S3E). Inactivation of *Fgf10* in the stromal niche, airway smooth muscle cells (ASMCs) and myofibroblasts, using *Acta2*^{CreERT2};*Fgf10*$^{f/f}$ mice, also blocks the generation of neo-BCs at the site of injury (Figures 2A, 2C, 2J, and 2K). Furthermore, we find a significant reduction in lung compliance 5–6 weeks after bleomycin injury in both *Scgb1a1*^{CreERT2};*Fgfr2b*$^{f/f}$ and *Acta2*^{CreERT2};*Fgf10*$^{f/f}$ mice compared with control littermates (Figures 2I, 2M, and S3E), indicating an impaired resolution of pulmonary fibrosis.

To verify that bronchial epithelial cells give rise to bona fide BCs and alveolar epithelial cells we performed single-cell transcriptome analysis on lineage-traced GFP^{+}, Tomato^{-}, CD45^{-}, and TER119^{-} isolated cells from uninjured and bleomycin injured *Sox2*^{CreERT2};*mTmG* lungs, which were treated with tamoxifen food for 3 weeks followed by a 2-month washout period. We identified GFP^{+} tuftt, hillock, ionocyte, club, goblet, neuroendocrine, UPK3a, and ciliated cells in both uninjured and injured lungs, yet only found basal, AT2 and AT1 cells in injured *Sox2*^{CreERT2};*mTmG* lungs (Figure 3). A heatmap for gene expression levels of the latter three cell types clearly shows segregation and enrichment for classical basal, AT2, and AT1 cell markers in each

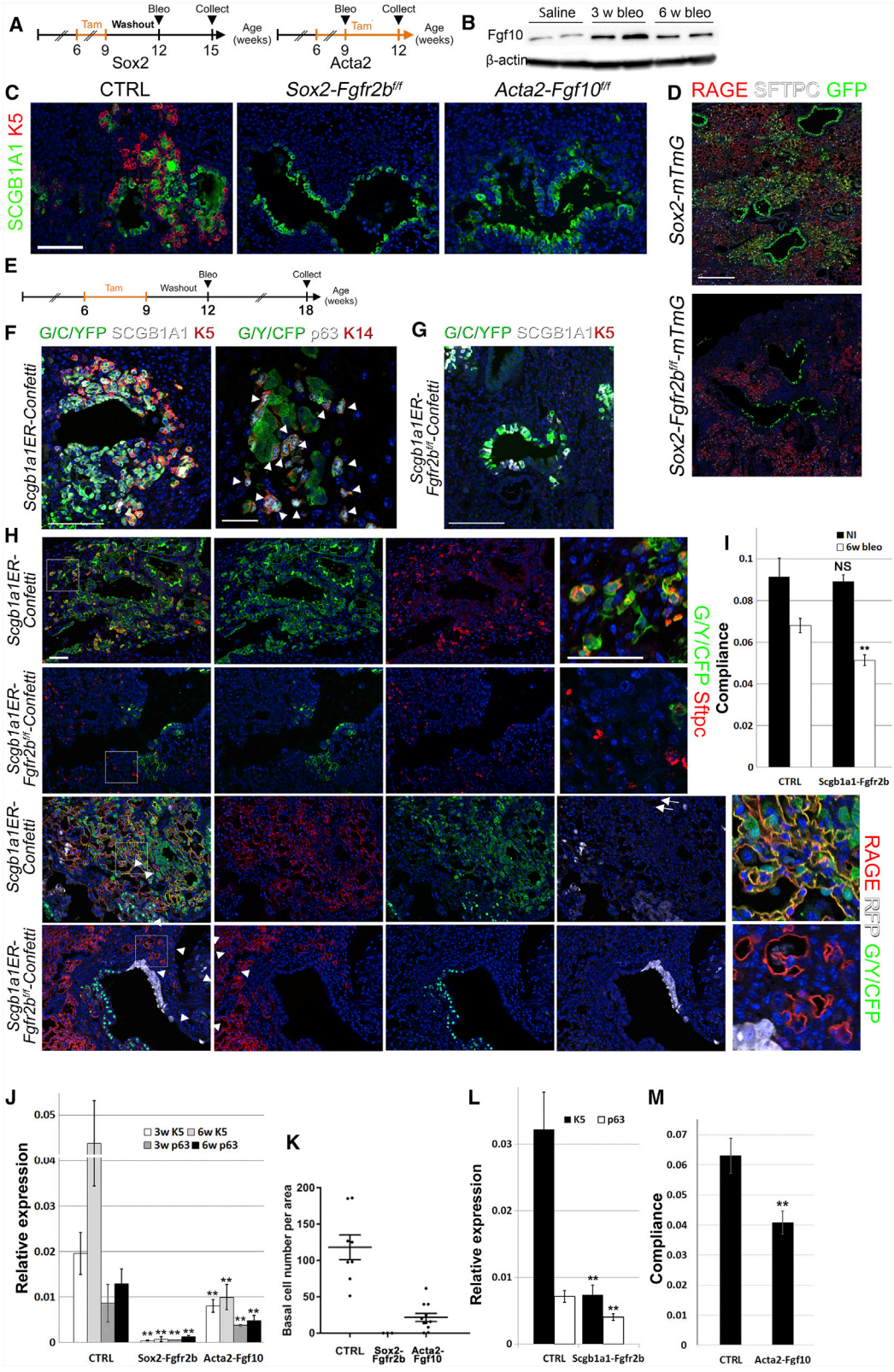

(legend on next page)

population, indicating that bronchial epithelial cells give rise to bona fide basal, AT2, and AT1 cells after bleomycin injury. Intriguingly, we found that AT2 cells express higher levels of *Fgfr2* than BCs suggesting a stronger dependence on FGF10 signaling. Unexpectedly, injured lungs also featured a distinct *de novo* previously undescribed ciliated cell population, which was *Gfp*$^{+}$, *Sox2*$^{+}$, *Foxj1*$^{+}$, but *Epcam*$^{-}$ and *E-cadherin*$^{-}$ (*Cdh1*). Together, our data demonstrate for the first time, to our knowledge, the crucial contribution of BESCs to alveolar epithelial regeneration and the resolution of pulmonary fibrosis after bleomycin injury, suggesting that BESCs may not merely be considered as a reserve stem cell population.

Overexpression of Fgf10 in Bronchial Epithelium Promotes the Generation of AT2 Cells over BCs

As our data suggest that FGF10-FGFR2B signaling is involved in BC generation and bronchiolization, as well as in alveolar epithelial regeneration, we questioned if the fate decision to either BCs or AT2 cells might depend on FGF10-FGFR2B signal strength. To investigate whether increased FGF10 signaling specifically in bronchial epithelial cells but not AT2 cells, promotes alveolar epithelial regeneration instead of bronchiolization, we generated *Sox2*^{CreERT2};*Rosa26-LSL-rtTA*;*Tet-Fgf10* mice, in which we can inducibly overexpress *Fgf10* specifically in bronchial epithelial cells and their descendants by placing mice on doxycycline chow. We found that overexpressing *Fgf10* in BESCs for 3 weeks starting 2 weeks after bleomycin injury pushed BESCs along the AT2 cell lineage (Figure 4A) resulting in a significant reduction in neo-BCs (Figure 4D). We further hypothesized that these new AT2 cells would differentiate into AT1 cells once *Fgf10* induction is terminated. To investigate this, we overexpressed *Fgf10* in BESCs for 3 weeks starting 2 weeks after bleomycin injury and harvested the lungs 1 week after *Fgf10* induction was stopped (i.e., 6 weeks after bleomycin injury). Our findings indeed showed that bronchial epithelial cells acquire an AT2 fate as long as *Fgf10* is overexpressed (Figure 4A). However, once *Fgf10* expression was stopped, some of the new AT2 cells spontaneously differentiated into AT1 cells (Figure 4B). Thus, our data highlight the importance of a strict temporally regulated regimen of *Fgf10* induction and suggest that FGF10 could be exploited as a novel therapeutic approach to promote alveolar epithelial regeneration in IPF patients by quickly and transiently boosting their endogenous stem cell population. Interestingly, our findings also suggest that overexpression of *Fgf10* results in a decrease in collagen deposition as measured by hydroxyproline levels (Figure 4C), and a significant reduction in neo-BCs (Figure 4D). These data are consistent with the idea that fibrosis is a wound-healing response that occurs when epithelial stem cells are exhausted.

Neo-BCs Exhibit Indeterminate States of Differentiation

Our findings suggest that FGF10-FGFR2B signaling in distal airway SCGB1A1^{+} cells drives both alveolar epithelial regeneration and bronchiolization following bleomycin injury. These findings further suggest the possibility that

Figure 2. Distal Bronchial Epithelial Cells Reprogram into Neo-BCs and AT1/2 Cells upon Bleomycin Injury in Response to Fgf10-Fgfr2b Signaling

(A) Experimental strategy of (C, J, and K).

(B) Western blotting for FGF10 on wild-type (wt) saline-treated lungs and wt lungs 3 and 6 weeks after bleomycin injury.

(C) Immunostaining on ctrl, *Sox2-Fgfr2b*$^{f/f}$, and *Acta2-Fgf10*$^{f/f}$ lungs for SCGB1A1 (green) and keratin 5 (K5) (red) at 3 weeks after bleomycin injury.

(D) Immunostaining on *Sox2-mTmG* and *Sox2-Fgfr2b*$^{f/f}$*-mTmG* lungs for SFTPC (white), RAGE (red), and GFP (green) at 6 weeks after bleomycin injury.

(E) Experimental strategy of (D and F–H).

(F) Immunostaining on *Scgb1a1ER-Confetti* lung for K5 (red), SCGB1A1 (white), or K14 (red), p63 (white), and G/Y/CFP (green) at 6 weeks after bleomycin injury. White arrowheads show K14, p63, and G/Y/CFP triple-positive cells, indicating the dedifferentiation of distal airway club cells into neo-BCs.

(G) Immunostaining on *Scgb1a1ER-Fgfr2bf/f-Confetti* lung for *Scgb1a1ER-Confetti* lung for K5 (red), SCGB1A1 (white), and G/Y/CFP (green), showing no basal cells near injury.

(H) Immunostaining on *Scgb1a1ER-Confetti* and *Scgb1a1ER-Fgfr2bf/f-Confetti* lungs for SFTPC (red), or RAGE (red) and RFP (white) and G/Y/CFP (green) (RFP and G/Y/CFP label the four different confetti clone cells) at 6 weeks after bleomycin injury.

(I) Flexivent pulmonary function analysis (static compliance) on ctrl and *Scgb1a1ER-Fgfr2b*$^{f/f}$ lungs 6 weeks after bleomycin injury.

(J) Relative mRNA levels of *K5* and *p63* in ctrl, *Sox2-Fgfr2b*$^{f/f}$, and *Acta2-Fgf10*$^{f/f}$ lungs 3 and 6 weeks after bleomycin injury.

(K) Quantification of BC numbers in ctrl, *Sox2-Fgfr2b*$^{f/f}$, and *Acta2-Fgf10*$^{f/f}$ lungs at 3 weeks after bleomycin injury.

(L) qPCR of relative mRNA levels of *K5* and *p63* in ctrl and *Scgb1a1ER-Fgfr2b*$^{f/f}$ lungs 6 weeks after bleomycin injury.

(M) Flexivent pulmonary function analysis (static compliance) on ctrl and *Acta2*^{CreERT2}*-Fgfr10*$^{f/f}$ lungs 5 weeks after bleomycin injury. Nuclei were stained with DAPI (blue).

$^{**}p < 0.01$, $^{*}p < 0.05$; $n \geq 14$; error bars mean ± SEM. Scale bars, 100 μm (C and H), 200 μm (F, left and G), 20 μm (F, right), 250 μm (D).

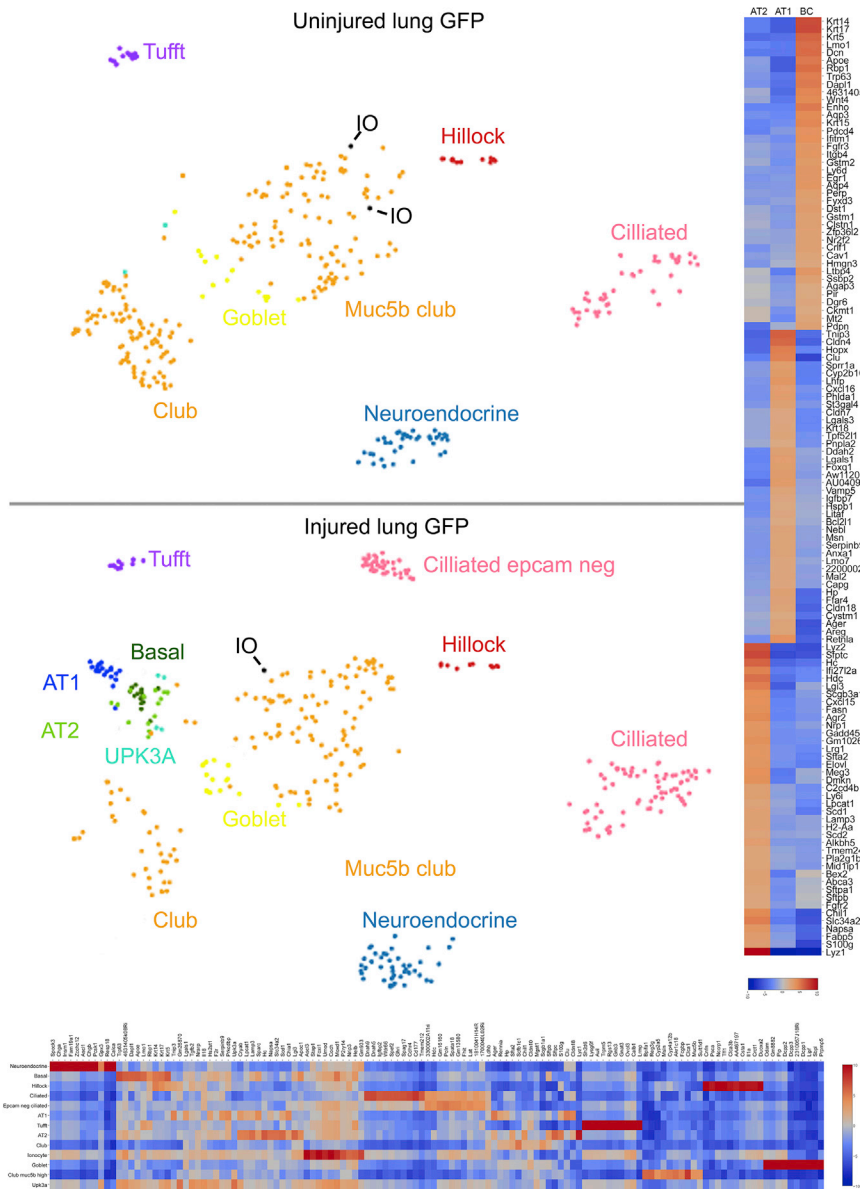

Figure 3. Single-Cell RNA-Seq Analysis of Lineage-Traced *Sox2*^{CreERT2};*mTmG* Cells 6 Weeks after Saline or Bleomycin Treatment

t-SNE plots show neuroendocrine cells, ciliated cells, hillock cells, tuft cells, ionocytes (IO), distal and proximal club cells, goblet cells, UPK3A cells, AT2, AT1, and BCs. Heatmaps show differential gene expression between the different subpopulations and/or AT1, AT2, and neo-BCs specifically highlighting cell-type signatures among both injured and uninjured lungs.

some bronchial epithelial cells may initially, transiently reprogram into neo-BCs before giving rise to alveolar epithelial cells. Interestingly, recent single-cell transcriptome analyses show that individual epithelial cells within bronchiolized honeycomb regions of IPF lungs frequently co-express AT1, AT2, basal, and other conducting airway selective markers, and even mesenchymal or epithelial-mesenchymal transition (EMT) markers, demonstrating "indeterminate" states of differentiation not seen during normal lung development or homeostasis (Gokey et al., 2018; Xu et al., 2016). Our data also suggest that some of the neo-BCs in bronchiolized regions in IPF or mouse lungs after bleomycin injury co-express basal (p63), and AT2 cell (SFTPC) markers or mesenchymal (alpha smooth muscle actin [α-SMA]) markers indicating that the same indeterminate states of differentiation observed in IPF also occur in mice after bleomycin injury (Figures 4E–4H and S4C).

It could be argued that these neo-BCs are derived from (broncho-alveolar stem cells [BASCs]) (Kim et al., 2005), which are club cells that co-express SCGB1A1^{+} and SFTPC^{+}. To explore this possibility we lineage-labeled AT2 cells and BASCs using an *Sftpc*^{CreERT2};*mTmG* mouse line. We found that labeling the BASCs required high doses of tamoxifen, likely because *Sftpc* expression is lower in these cells than in AT2 cells. With lower doses of tamoxifen administration only AT2 cells were labeled (Figures S4A and S4B). Interestingly, we found that, when only AT2 cells were labeled before bleomycin injury, none of the neo-BCs that arose after injury were GFP^{+} (Figure S4A). However, when BASCs were labeled before injury neo-BCs were also lineage labeled (Figures 4I and 4J). Note that the lineage-labeled cells are SCGB1A1^{+} and K5^{+}.

Our data further suggest that some neo-BCs that appear after bleomycin injury transiently express the mesenchymal marker α-SMA (Figure 4H) approximately 2 weeks after injury. This is indicative of a partial EMT-like migratory phenotype, and is remarkably similar to myoepithelial cells, a stem cell population located in the submucosal glands (Anderson et al., 2017; Lynch et al., 2016; Volckaert and De Langhe, 2014), which also co-express BC (K5, p63) and mesenchymal markers (α-SMA) (Lynch et al., 2018; Tata et al., 2018). Interestingly, we previously reported how FGF10-FGFR2B signaling induces a partial

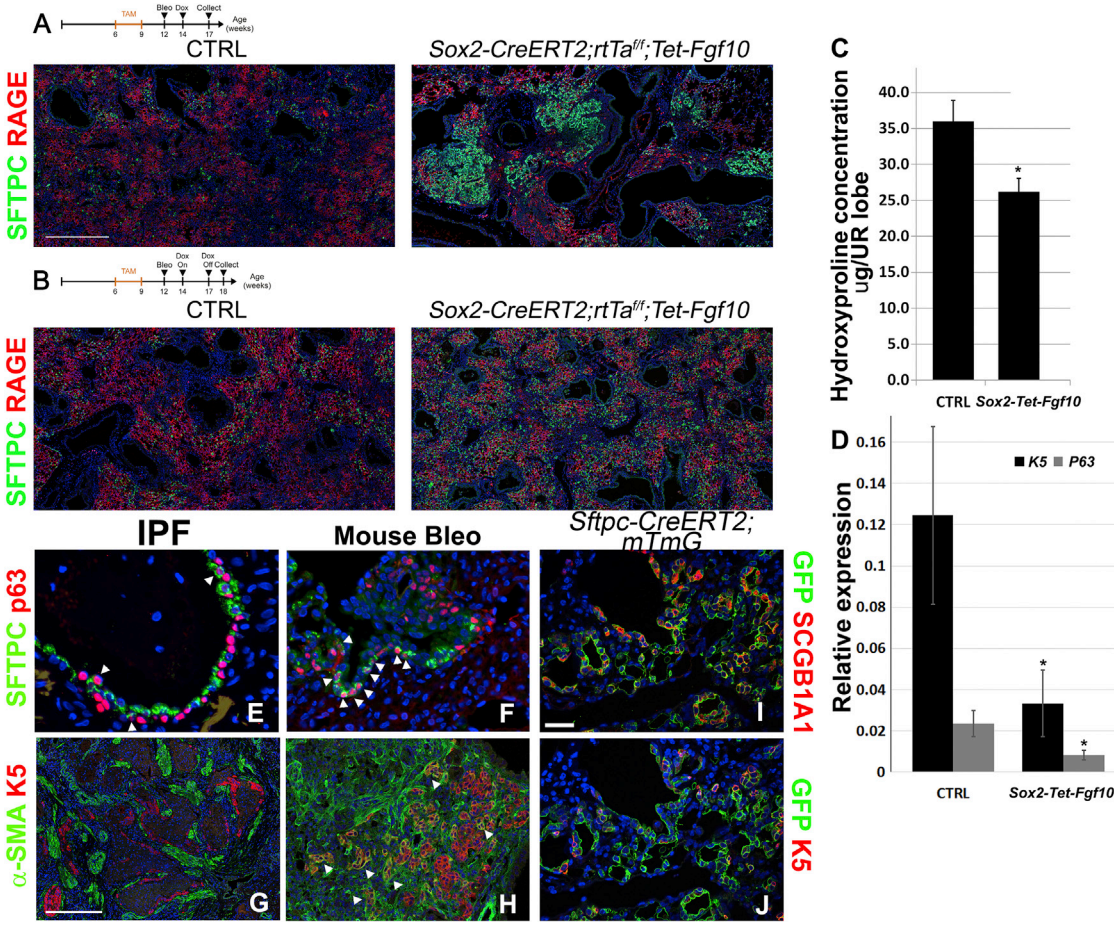

Figure 4. Overexpression of *Fgf10* in Bronchial Epithelial Cells after Bleomycin Injury Promotes AT2 Cell Differentiation

(A and B) Coimmunostaining for RAGE (AT1 cell) and/or SFTPC (AT2 cell) on *Sox2*^{CreERT2};*LSL-rtTa;Tet-Fgf10* lungs that received intratracheal bleomycin at 2 months of age and were placed on doxycycline-containing chow 2 weeks after bleomycin injury for 3 weeks and were harvested either at 5 (A) or 6 (B) weeks after injury.

(C) Hydroxyproline measurements for collagen content in ctrl and Sox2CreERT2; LSL-*rtTa;Tet-Fgf10* mice 6 weeks after bleomycin injury ($n \geq 15$).

(D) Relative mRNA levels of *K5*, *p63* in ctrl and *Sox2*^{CreERT2};*LSL-rtTa;Tet-Fgf10* mice 6 weeks after bleomycin injury ($n \geq 15$).

(E–J) Coimmunostaining for SFTPC (green) and p63 (red) (E and F) or α-SMA (green) and K5 (red) and (G and H) on honeycomb regions in lungs from IPF patients and mouse lungs 18 days after bleomycin injury. White arrowheads (E and F) show SFTPC and p63 double-positive cells. (I and J) Immunostaining on *Sftpc*^{CreERT2};*mTmG* lungs for SCGB1A1 (red) or K5 (red) and GFP (green) at 3 weeks after bleomycin injury. Nuclei were stained with DAPI (blue). White arrowheads (H) show α-SMA (green) and K5 (red) double-positive cells.

*$p < 0.05$; $n \geq 14$; error bars mean ± SEM. Scale bars, 500 μm (A and B), 100 μm (G and H), and 50 μm (E, F, I, and J).

EMT-like phenotype in a subset of club cells that drive airway epithelial regeneration after naphthalene injury (Volckaert et al., 2011). While single-cell transcriptomics has identified a population of indeterminate epithelial cells with mesenchymal traits in IPF lungs (Xu et al., 2016), we have not yet been able to visualize K5$^+$ α-SMA$^+$ double-positive cells in IPF lungs (Figure 4G). This suggests the possible transient nature of these "elusive" cells, which may be more abundant during the early stages of disease.

FGFR2B Signaling Is Required for Neo-BCs to Differentiate into AT2 Cells during the Resolution of Bleomycin IPF

To investigate the possibility that some neo-BCs might be able to differentiate into alveolar epithelial cells during the resolution of bleomycin-mediated injury in mice, we lineage-traced neo-BCs after bleomycin injury using *Krt5*^{CreERT2};*mTmG* mice (with tamoxifen treatment starting at 17 days after bleomycin injury; because the first neo-BCs only appear 14 days after injury). When we followed the

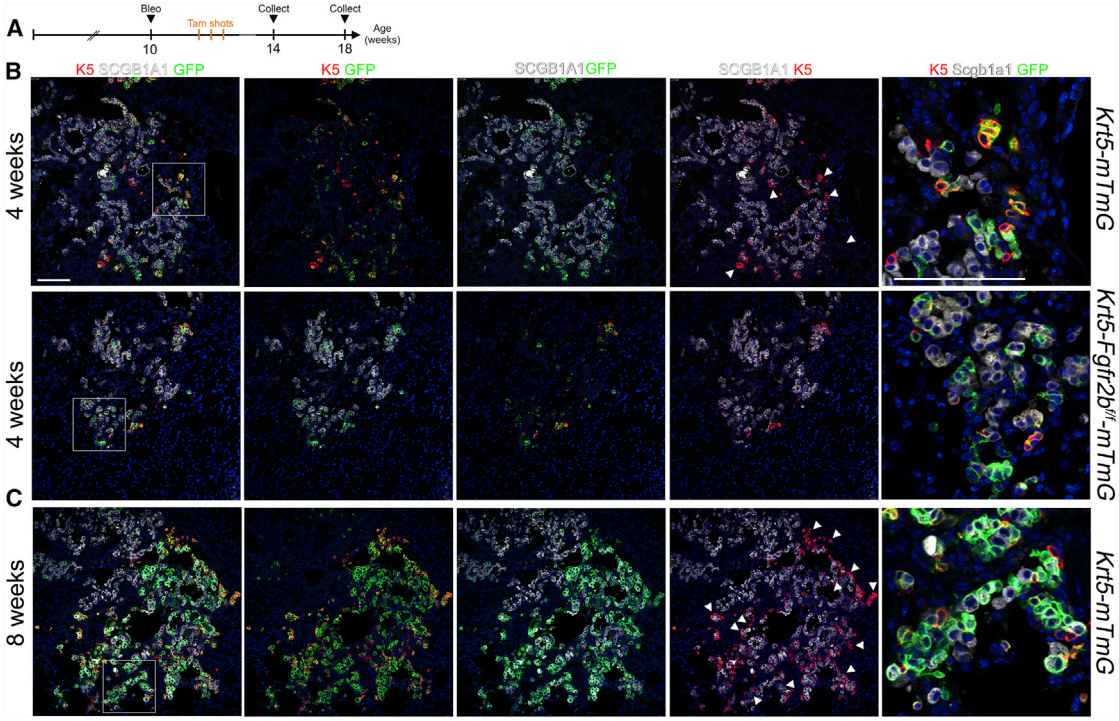

Figure 5. Neo-BCs Require Fgfr2b Signaling for their Maintenance

(A) Experimental strategy of (B). Induction with tamoxifen was performed at days 17, 19, and 21 after bleomycin injury.

(B and C) Immunostaining on *Krt5-mTmG* lungs and *Krt5-Fgfr2b*$^{f/f}$*-mTmG* lungs to localize keratin 5 (K5) (red), SCGB1A1 (white), and GFP (green) (left) at 4 (B) or 8 weeks (C) after bleomycin injury. White arrowheads (B and C) show K5 (red) positive and SCGB1A1 (white) negative cells. Nuclei were stained with DAPI (blue). Scale bars, 100 μm (B and C).

fate of these cells to 11 days or 4 weeks after bleomycin injury, we found that ~65% of the GFP-labeled cells were still positive for KRT5 and p63; however, ~35% of GFP-labeled cells no longer expressed these BC markers. Interestingly, we found that, at 4 weeks after bleomycin injury, ~13% of GFP$^+$ cells were positive for the AT1 cell marker RAGE, whereas about ~4% stained positive for SFTPC, an AT2 cell marker (Figures 5A, 5B, and 6A–6C). Intriguingly, we also found that ~81% of GFP$^+$ cells were positive for SCGB1A1, a club cell marker (Figures 5A, 5B, and 6A–6C), again indicating that neo-BCs that appear after bleomycin injury are derived from *Sox2*$^+$*/Scgba1a1*$^+$ bronchial epithelial cells or that these BCs also give rise to club cells. As fibrosis resolution is not complete by 4 weeks after bleomycin injury, we lineage traced these cells until 8 weeks after injury. At 8 weeks after bleomycin injury, only ~35% of GFP$^+$ cells still expressed BC markers, whereas ~28% of GFP$^+$ cells had differentiated into RAGE$^+$ AT1 cells, and ~9% had differentiated in SFTPC$^+$ AT2 cells (Figures 5A, 5C, 6A–6C, and S5). Interestingly, ~49% of GFP$^+$ cells stained for SCGB1A1 at 8 weeks after bleomycin injury.

A time course of BC abundance after bleomycin injury further indicated that neo-BCs first appeared in the parenchyma around 2 weeks after injury (not shown) and peaked at around 4–6 weeks after injury after which their numbers slowly declined (Figure 6D). However, when total lung *Gfp* expression levels were measured we observed a trend toward increased *Gfp* levels (and GFP$^+$ cells) at 8 weeks after bleomycin injury compared with 4 weeks after bleomycin injury (Figure 6E) suggesting that the lineage-labeled neo-BCs can differentiate and that their offspring persists, contributing to alveolar epithelial regeneration.

We next hypothesized that FGF10-FGFR2B signaling could also be required for the maintenance of these neo-BCs after bleomycin injury as well as their subsequent differentiation into AT1 and AT2 cells. To investigate this we inactivated *Fgfr2b* in bleomycin injury-induced neo-BCs using *Krt5*^{CreERT2}*;Fgfr2b*$^{f/f}$*;Rosa26*^{mTmG} mice. Interestingly, these mice die around 30 days after bleomycin injury or 13 days after inactivation of FGFR2B. By 4 weeks after injury we found a strong reduction in *Krt5* and *p63* expression, suggesting decreased BCs, but not in lineage-labeled *Gfp* expression, suggesting that FGFR2B signaling is also required for neo-BC maintenance (Figure 6E). Consistently, we found that at 4 weeks after bleomycin injury, only ~39% of the GFP-labeled cells in *Krt5-Fgfr2b*$^{f/f}$*-mTmG* lungs

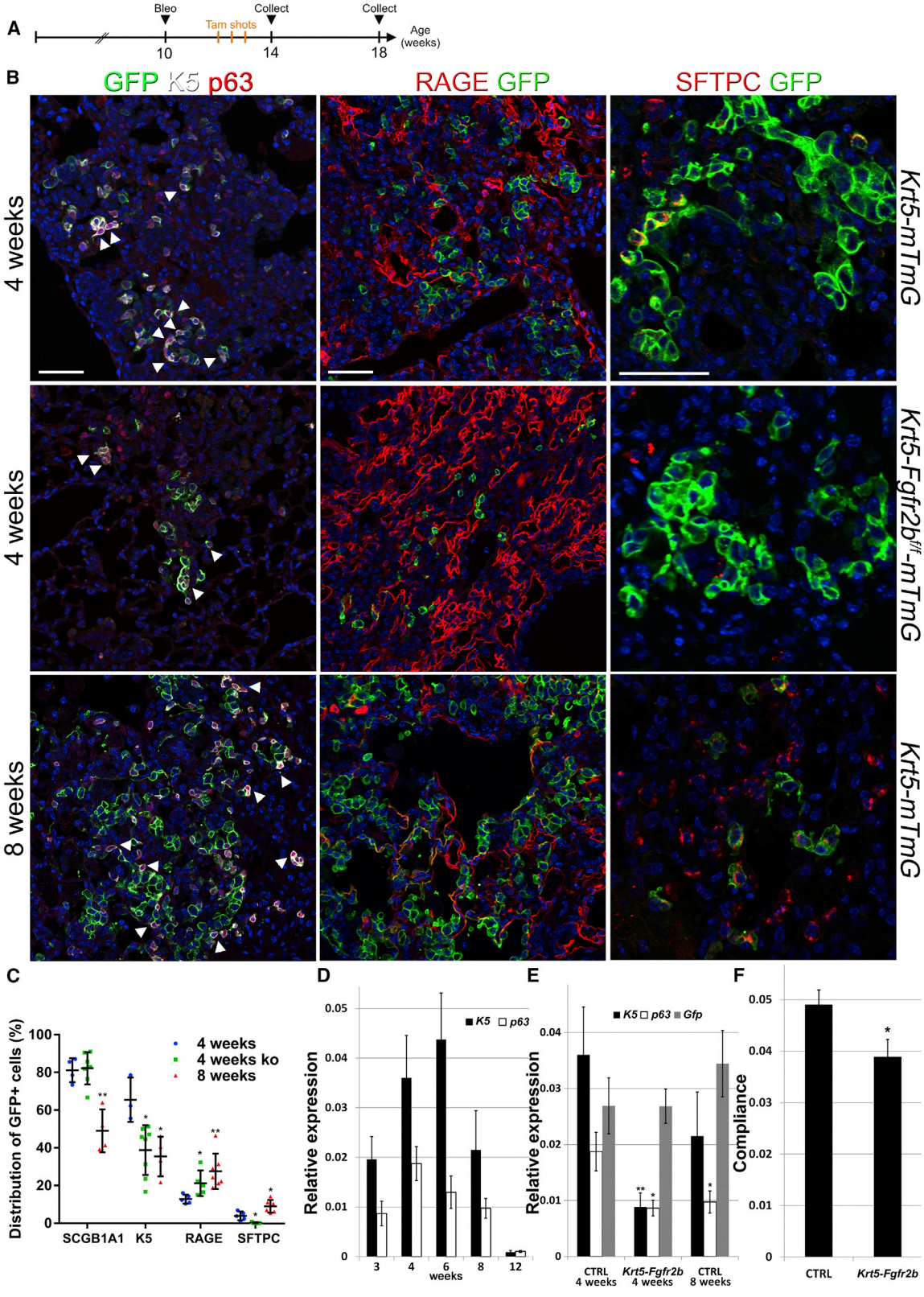

(legend on next page)

remain positive for KRT5, whereas ~21% of GFP$^+$ cells differentiated into RAGE$^+$ AT1 cells, while none of the GFP$^+$ cells had differentiated into AT2 cells (Figures 6A–6C). The lack of AT2 cell differentiation is consistent with a requirement for FGF10-FGFR2B signaling in AT2 cell maintenance (Figure 1F). Interestingly, similar to control mice, ~82% of GFP-labeled cells were positive for SCGB1A1 (Figures 5A, 5B, and 6A–6C). Furthermore, pulmonary function testing indicated that *Krt5^{CreERT2};Fgfr2b$^{f/f}$;mTmG* mice, whereby we effectively inactivated *Fgfr2b* in neo-BCs after bleomycin injury, showed a significant reduction in static lung compliance compared with control mice 4 weeks after bleomycin injury, suggestive of impaired resolution of pulmonary fibrosis (Figure 6F). These data, therefore, suggest that neo-BCs play a regenerative role following lung injury, by slowly giving rise to AT1 and AT2 cells and that FGFR2B signaling is required for their maintenance and proper differentiation.

In summary, our data suggest that FGF10-FGFR2B signaling drives the reprogramming of *p63$^+$/Scgb1a1$^+$/Sox2$^+$* BESCs in the distal airway into neo-BCs after bleomycin injury and their further differentiation into AT1 and AT2 cells. When FGF10-FGFR2B signaling is inhibited before injury, neo-BCs are not generated, leaving behind large cystic structures arising as a result of impaired alveolar epithelial regeneration by conducting airway epithelium (Figure S3E). Our data also suggest that FGF10-FGFR2B signaling is required for the maintenance of these injury-induced neo-BCs, some of which differentiate back into club cells or slowly give rise to AT1 but not AT2 cells when FGF10-FGFR2B signaling is abrogated.

Translation Significance of FGF10 Signaling in Human IPF Lung Slices in which FGF10 Promotes the Differentiation of BCs in Honeycomb Cysts along the AT2 Lineage

Based on our findings in mice we further validated a role for FGF10 signaling in the reprogramming of BCs within honeycomb cysts in IPF tissue along the AT2 cell lineage. To assess the potential for FGF10 to reprogram the BCs in the honeycomb cysts of IPF patients into AT2 cells we cultured live precision cut IPF lung slices in the presence or absence of FGF10. Treatment with FGF10 resulted in a ~1.6-fold in CK5$^-$ HTII-280$^+$ AT2 cells and a 1.5-fold increase in CK5$^+$ HTII-280$^+$ double-positive cells versus a 13% decrease in CK5$^+$ HTII-280$^-$ BCs after FGF10 treatment, supporting the concept that FGF10 signaling can push BCs in IPF tissue along the AT2 cell lineage (Figure 7A).

DISCUSSION

The major finding of our study is that upon acute bleomycin-mediated lung injury, FGF10-FGFR2B signaling generates BCs and drives alveolar epithelial regeneration by BESCs to promote the resolution of pulmonary fibrosis (Figures 7B and 7C). Upon airway epithelial injury, ASMCs, which wrap the conducting airways, as well as myofibroblasts, are activated and release FGF10 to become an injury-induced stem/progenitor cell niche. FGF10 from the stromal niche drives the dedifferentiation of distal airway club cells into neo-BCs and alveolar epithelial cells. Interestingly our data suggest that FGF10/FGFR2B signaling is necessary to maintain and amplify the pool of neo-BCs and that it is critical to drive their differentiation into AT2 cells, whereas in the absence of FGFR2B signaling these neo-BCs primarily give rise to AT1 cells. This is consistent with our findings that FGF10-FGFR2B signaling is essential for AT2 stem cell maintenance.

Our lineage-tracing data argue that the induction of *Fgf10* expression by the stromal niche allows for the dedifferentiation of a subset of distal airway club cells. As such, we found that basal stem/progenitor cells were lineage labeled within each clonal expansion and dispersal of labeled club daughter cells into the alveoli of *Scgb1a1^{CreER};Confetti* lungs. In addition, when neo-BCs were lineage tagged after bleomycin injury using *Krt5-mTmG* mice, ~80% were found to co-express the club cell marker SCGB1A1. These findings are consistent with recent reports (Yang et al., 2018).

Our finding that FGF10-FGFR2B signaling is critical for club cell dedifferentiation and subsequent differentiation into alveolar epithelial cells allowed us for the first time

Figure 6. BCs that Appear through Reprogramming of Scgb1a1$^+$ Cells after Bleomycin Injury Require Fgfr2b Signaling for their Maintenance and to Differentiate into Alveolar Epithelial Cells

(A) Experimental strategy of (B–F). Tamoxifen induction was performed on days 17, 19, and 21 after bleomycin injury.

(B) Immunostaining on *Krt5-mTmG* lungs and *Krt5-Fgfr2b$^{f/f}$-mTmG* lungs for p63 (red), K5 (white), and GFP (green) or RAGE (red) and GFP (green) (middle) or SFTPC (red) and GFP (green) (right) at 4 and/or 8 weeks after bleomycin injury. White arrowheads show p63 (red), K5 (white), and GFP (green) triple-positive cells.

(C) Quantification of the distribution of GFP$^+$ cells in (B).

(D) Relative mRNA levels of *K5* and *p63* at 3, 4, 6, 8, and 12 weeks after bleomycin injury showing time course of BC abundance.

(E) Relative mRNA levels of *K5*, *p63*, and *Gfp* in control and *Krt5-Fgfr2b$^{f/f}$* lungs at 4 weeks after bleomycin injury.

(F) Flexivent pulmonary function analysis measured static compliance on control and *Krt5-Fgfr2b$^{f/f}$* lungs at 4 weeks after bleomycin injury.

Nuclei were stained with DAPI (blue). $^{**}p < 0.01$, $^{*}p < 0.05$; $n \geq 14$; error bars mean ± SEM. Scale bars, 50 μm (B).

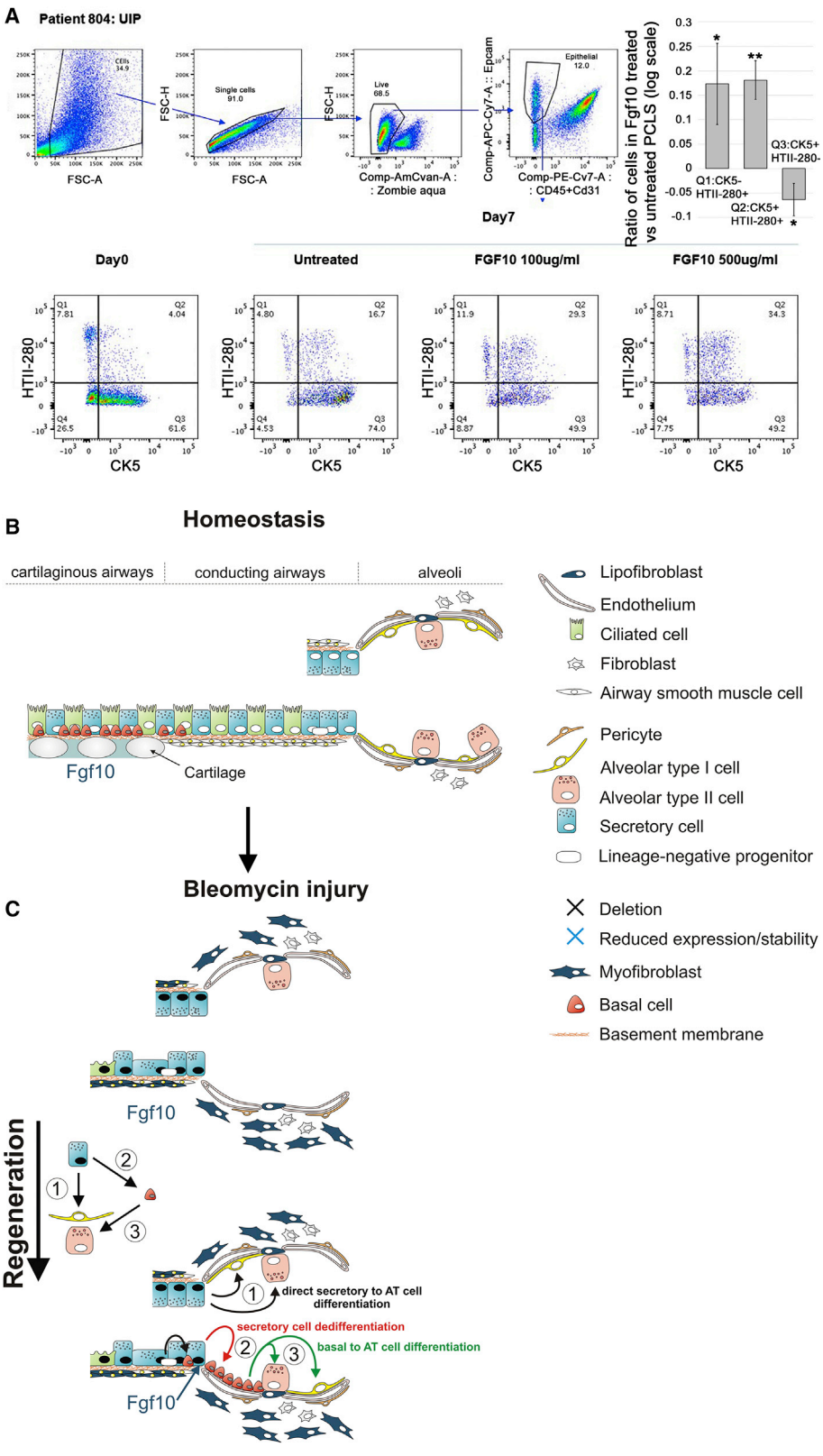

(legend on next page)

to investigate the importance of these distal airway club cells or BASCs (Kim et al., 2005) in alveolar epithelial regeneration. Our data suggest for the first time that under normal conditions BESCs do play an essential role in alveolar epithelial regeneration. This is particularly intriguing because these cells are also the source of Muc5b, which has been associated with the development of pulmonary fibrosis (Nakano et al., 2016; Seibold et al., 2011).

With age, *Fgf10* expression goes down and our data strongly suggest that in young lungs FGF10-FGFR2B signaling drives the reprogramming of bronchial epithelial cells into alveolar epithelial cells, and that FGF10 treatment can possibly help misguided BCs in honeycomb cysts in IPF tissue along the right path. However, we believe that this process does not take place in patients with IPF likely because *Fgf10* expression goes down with age. It is to be hoped that these novel findings will result in new therapeutic options for the treatment of IPF.

Finally, the bleomycin mouse model for modeling human IPF has its pros and cons. For a long time, the mouse bleomycin model was not thought to generate honeycomb cysts-like structures. However, bronchiolarization and the appearance of BCs only occurs upon severe or repetitive bleomycin injury and is not observed under conditions of mild injury. The bleomycin mouse model in young mice also resolves over time, which allows us to study the regenerative capacity of the different epithelial stem cells. While human IPF is a fatal disease that does not resolve, it is also a disease of aging and stem cell exhaustion. It is therefore likely that the capacity to recover from injury also diminishes with time in humans.

EXPERIMENTAL PROCEDURES

Experimental Model and Subject Details

All mice were bred and maintained in a pathogen-free environment with free access to food and water. Both male and female mice were used for all experiments. *Fgfr2b*$^{f/f}$ (De Moerlooze et al., 2000), *Sox2*^{CreERT2} (JAX 017593), *Tet-Fgf10* (Clark et al., 2001), *Rosa26-rtTa* (Volckaert et al., 2011), *Rosa26-rtTa*$^{f/f}$ (JAX 005670), Rosa26 *Rosa26*R-*Confetti* (JAX 017492), *Scgb1a1*^{CreER} (JAX 016225), *Rosa26*-mTmG (JAX 007676), *Krt5*^{CreERT2} (Van Keymeulen et al., 2011), *Acta2*^{CreERT2} (Wendling et al., 2009), *Fgf10*$^{f/f}$ (Urness et al., 2010), *Sftpc*^{CreERT2} (Chapman et al., 2011), and *Fgf10*^{LacZ} (Kelly et al., 2001) mice have been described.

For bleomycin injury, adult 8- to 12-week-old mice were intratracheally instilled with 50 μL bleomycin (0.8–2 U/kg body weight optimized for each strain, batch of bleomycin, and gender) as described previously (Redente et al., 2014). Lung function was analyzed using lung measurements of static compliance by Flexivent (SQIREQ). Bleomycin injury was induced after a 21-day washout period following tamoxifen induction. For tamoxifen induction, mice were placed on tamoxifen-containing food (rodent diet with 400 mg/kg tamoxifen citrate; Harlan Teklad TD.130860) for 2 to 3 weeks. *Scgb1a1*^{CreER};*Fgfr2b*$^{f/f}$;*Rosa26*R-*Confetti* and control mice also received two additional intraperitoneal tamoxifen citrate shots (0.20 mg/g body weight, Enzo Life Sciences) in the last week of tamoxifen citrate feed. *Krt5CreER;Fgfr2b*$^{f/f}$;*Rosa26*-mTmG and control mice received intraperitoneal tamoxifen citrate shots (0.125 mg/g body weight) on day 17, 19, and 21 after bleomycin injury. For doxycycline induction: mice were placed on doxycycline-containing food (rodent diet with 625 mg/kg dox; Harlan Teklad TD.09761). All experiments were approved by the National Jewish Health and University of Alabama at Birmingham Institutional animal care and use committee.

Single-Cell RNA-Seq

Sox2^{CreERT2};*mTmG* mice were placed on tamoxifen food for 3 weeks starting at 2 months of age, followed by a 2-month washout period before saline or bleomycin treatment. Whole lung tissues were collected, from lineage-traced mice 6 weeks after saline or bleomycin treatment. Single cells were processed through the GemCode Single Cell Platform using the GemCode Gel Bead, Chip and Library Kits (V1) or single-cell suspensions were loaded onto 3′ library chips for the Chromium Single Cell 3′ Library (V2, PN-120267) according to the manufacturer's recommendations (10X Genomics). Libraries were sequenced on an Illumina NextSeq 500 at >190,000 reads per cell. Further details on single-cell RNA-seq analysis and the fluorescence-activated cell sorting (FACS) protocol can be found in the Supplemental Experimental Procedures.

Immunofluorescence Microscopy and qRT-PCR

Details of all immunostaining protocols, antibodies employed, and quantitation of gene expression by qRT-PCR are provided in the Supplemental Experimental Procedures.

Microscopy and Imaging

Tissue was imaged using a micrometer slide calibrated Zeiss LSM800 Laser scanning confocal microscope using ZEN imaging software. In

Figure 7. BCs in Precision Cut IPF Lung Slices Treated with Fgf10 Differentiate into AT2 Cells

(A) Flow sorting for alveolar AT2 marker HTII-280 and CK5 on precision-cut lung slices cultured in the absence or presence of FGF10. Graph displayed as the log of the fold change shows an increase in CK5$^-$ HTII-280$^+$ and CK5$^+$ HTII-280$^+$ double-positive cells but a decrease in CK5$^+$ HTII-280$^-$ cells after FGF10 treatment. **p < 0.01, *p < 0.05; n = 5; error bars mean ± SEM.

(B and C) Model showing how FGF10-FGFR2B maintains and generates basal-like stem cells by activating the stromal niche during homeostasis and epithelial regeneration. (B) During homeostasis, BCs are only found in the trachea, where they depend on FGF10 secreted by the intercartilage stromal tissue. (C) The dedifferentiation of distal airway club cells after major lung epithelial injury critically depends on FGF10-FGFR2B signaling. Note that, in addition to *Fgf10*-expressing ASMCs, activated myofibroblasts may further provide a strong additional source of FGF10 to allow for BC mobilization to injured regions. At injured sites, neo-BCs give rise to AT cells.

the lung, cells were counted using tiled stitched 20× images covering the entire cross-section of the left lung lobe from ≥6 different lungs. Images were processed and analyzed using ZEN blue (Zeiss) and Adobe Photoshop Creative Suite 3 (Adobe) software. Differentiation of GFP^+ cells was determined by quantifying the total number of GFP^+ cells that also showed a DAPI-stained nucleus, and how many of those were RAGE, K5, p63, or $SFTPC^+$. Image quantification and analysis were performed in a double-blinded fashion.

Precision Cut Lung Slices

Human lung tissues from non-IPF donors and IPF patients undergoing lung transplantation were obtained from the Giessen biobank. The study protocol was approved by the ethics committee of the University of Giessen that conforms to the principles outlined in the declaration of Helsinki.

Vibratome slices (400 μm) were made from low melting agarose filled de-identified human IPF transplant lung tissue. Precision cut lung slices were then cultured at the air-liquid interface in RPMI +10% Human Serum (Seraclot), ITS, Pen/Strep, Amphotericin B in the presence or absence of 500 ng/mL FGF10 for 3 to 7 days. Subsequently, slices were analyzed via FACS for basal (Abcam and AT2; Terrace Biotech, HT2-280, 1:150) cell markers.

Quantification and Statistical Analysis

All results are expressed as mean values ± SEM. The "n" represents biological replicates and can be found in the figure legends. The significance of differences between two sample means was determined by unpaired Student's t-test (assuming unequal or equal variances as determined by the F test of equality of variances). All datasets followed a normal distribution and p values < 0.05 were considered statistically significant. The number of samples to be used was based on the number of experimental paradigms multiplied by the number in each group that is necessary to yield statistically significant results based on power analysis, to reject the null hypothesis with 80% power (type I error = 0.05).

ACCESSION NUMBERS

The accession number for the raw data files of RNA-seq analyses reported in this paper is GEO: GSE129079.

SUPPLEMENTAL INFORMATION

Supplemental Information can be found online at https://doi.org/10.1016/j.stemcr.2019.04.003.

AUTHOR CONTRIBUTIONS

T.Y. and T.V. designed and performed the experiments, analyzed the data, and wrote and edited the manuscript. E.F.R., S.H., K.K., R.W., J.Y., C.-M.C., B.R.S., and C.Y. performed the experiments. E.F.R., J.-S.Z., S.M., B.R.S., A.G., D.W.H.R., S.B., and V.J.T. edited the manuscript. S.P.D.L. conceived and led the project, performed experiments, analyzed data, and wrote and edited the manuscript.

ACKNOWLEDGMENTS

This study was supported by NIH R01 HL107307, DFG (BE443/4-1 and BE443/6-1), Loewe and UKGM (to S.B.), VA-CDA 1IK2BX002401-01A2 (to E.R.), NIH R01 HL140595 and VA Merit I01 BX003471 (to D.R.), NIH RO1 HL135163 and PO1 HL108793 (to B.R.S.), and NIH R01 HL126732, HL132156, HL146461, and the Pulmonary Fibrosis Foundation Albert Rose established investigator award to S.D.L.

Received: March 3, 2017
Revised: April 1, 2019
Accepted: April 2, 2019
Published: May 2, 2019

REFERENCES

Anderson, P.J., Lynch, T.J., and Engelhardt, J.F. (2017). Multipotent myoepithelial progenitor cells are born early during airway submucosal gland development. Am. J. Respir. Cell Mol. Biol. *56*, 716–726.

Balasooriya, G.I., Goschorska, M., Piddini, E., and Rawlins, E.L. (2017). FGFR2 is required for airway basal cell self-renewal and terminal differentiation. Development *144*, 1600–1606.

Barkauskas, C.E., and Noble, P.W. (2014). Cellular mechanisms of tissue fibrosis. 7. New insights into the cellular mechanisms of pulmonary fibrosis. Am. J. Physiol. Cell Physiol. *306*, C987–C996.

Barkauskas, C.E., Cronce, M.J., Rackley, C.R., Bowie, E.J., Keene, D.R., Stripp, B.R., Randell, S.H., Noble, P.W., and Hogan, B.L. (2013). Type 2 alveolar cells are stem cells in adult lung. J. Clin. Invest. *123*, 3025–3036.

Camelo, A., Dunmore, R., Sleeman, M.A., and Clarke, D.L. (2014). The epithelium in idiopathic pulmonary fibrosis: breaking the barrier. Front. Pharmacol. *4*, 173.

Chanda, D., Kurundkar, A., Rangarajan, S., Locy, M., Bernard, K., Sharma, N.S., Logsdon, N.J., Liu, H., Crossman, D.K., Horowitz, J.C., et al. (2016). Developmental reprogramming in mesenchymal stromal cells of human subjects with idiopathic pulmonary fibrosis. Sci. Rep. *6*, 37445.

Chapman, H.A., Li, X., Alexander, J.P., Brumwell, A., Lorizio, W., Tan, K., Sonnenberg, A., Wei, Y., and Vu, T.H. (2011). Integrin alpha6beta4 identifies an adult distal lung epithelial population with regenerative potential in mice. J. Clin. Invest. *121*, 2855–2862.

Clark, J.C., Tichelaar, J.W., Wert, S.E., Itoh, N., Perl, A.K., Stahlman, M.T., and Whitsett, J.A. (2001). FGF-10 disrupts lung morphogenesis and causes pulmonary adenomas in vivo. Am. J. Physiol. Lung Cell Mol. Physiol. *280*, L705–L715.

El Agha, E., Moiseenko, A., Kheirollahi, V., De Langhe, S., Crnkovic, S., Kwapiszewska, G., Kosanovic, D., Schwind, F., Schermuly, R.T., Henneke, I., et al. (2017). Two-way conversion between lipogenic and myogenic fibroblastic phenotypes marks the progression and resolution of lung fibrosis. Cell Stem Cell *20*, 261–273.e3.

Evans, C.M., Williams, O.W., Tuvim, M.J., Nigam, R., Mixides, G.P., Blackburn, M.R., DeMayo, F.J., Burns, A.R., Smith, C., Reynolds, S.D., et al. (2004). Mucin is produced by Clara cells in the proximal airways of antigen-challenged mice. Am. J. Respir. Cell Mol. Biol. *31*, 382–394.

Gokey, J.J., Sridharan, A., Xu, Y., Green, J., Carraro, G., Stripp, B.R., Perl, A.T., and Whitsett, J.A. (2018). Active epithelial Hippo signaling in idiopathic pulmonary fibrosis. JCI Insight *3*. https://doi.org/10.1172/jci.insight.98738.

Guha, A., Deshpande, A., Jain, A., Sebastiani, P., and Cardoso, W.V. (2017). Uroplakin 3a+ cells are a distinctive population of epithelial progenitors that contribute to airway maintenance and post-injury repair. Cell Rep. *19*, 246–254.

Hancock, L.A., Hennessy, C.E., Solomon, G.M., Dobrinskikh, E., Estrella, A., Hara, N., Hill, D.B., Kissner, W.J., Markovetz, M.R., Grove Villalon, D.E., et al. (2018). Muc5b overexpression causes mucociliary dysfunction and enhances lung fibrosis in mice. Nat. Commun. *9*, 5363.

Kelly, R.G., Brown, N.A., and Buckingham, M.E. (2001). The arterial pole of the mouse heart forms from Fgf10-expressing cells in pharyngeal mesoderm. Dev. Cell *1*, 435–440.

Van Keymeulen, A., Rocha, A.S., Ousset, M., Beck, B., Bouvencourt, G., Rock, J., Sharma, N., Dekoninck, S., and Blanpain, C. (2011). Distinct stem cells contribute to mammary gland development and maintenance. Nature *479*, 189–193.

Kim, C.F., Jackson, E.L., Woolfenden, A.E., Lawrence, S., Babar, I., Vogel, S., Crowley, D., Bronson, R.T., and Jacks, T. (2005). Identification of bronchioalveolar stem cells in normal lung and lung cancer. Cell *121*, 823–835.

King, T.E., Jr., Pardo, A., and Selman, M. (2011). Idiopathic pulmonary fibrosis. Lancet *378*, 1949–1961.

Klar, J., Blomstrand, P., Brunmark, C., Badhai, J., Hakansson, H.F., Brange, C.S., Bergendal, B., and Dahl, N. (2011). Fibroblast growth factor 10 haploinsufficiency causes chronic obstructive pulmonary disease. J. Med. Genet. *48*, 705–709.

Kropski, J.A., Blackwell, T.S., and Loyd, J.E. (2015). The genetic basis of idiopathic pulmonary fibrosis. Eur. Respir. J. *45*, 1717–1727.

Kumar, P.A., Hu, Y., Yamamoto, Y., Hoe, N.B., Wei, T.S., Mu, D., Sun, Y., Joo, L.S., Dagher, R., Zielonka, E.M., et al. (2011). Distal airway stem cells yield alveoli in vitro and during lung regeneration following H1N1 influenza infection. Cell *147*, 525–538.

Lee, J.H., Bhang, D.H., Beede, A., Huang, T.L., Stripp, B.R., Bloch, K.D., Wagers, A.J., Tseng, Y.H., Ryeom, S., and Kim, C.F. (2014). Lung stem cell differentiation in mice directed by endothelial cells via a BMP4-NFATc1-thrombospondin-1 axis. Cell *156*, 440–455.

Li, S., Wang, Y., Zhang, Y., Lu, M.M., DeMayo, F.J., Dekker, J.D., Tucker, P.W., and Morrisey, E.E. (2012). Foxp1/4 control epithelial cell fate during lung development and regeneration through regulation of anterior gradient 2. Development *139*, 2500–2509.

Lynch, T.J., Anderson, P.J., Xie, W., Crooke, A.K., Liu, X., Tyler, S.R., Luo, M., Kusner, D.M., Zhang, Y., Neff, T., et al. (2016). Wnt signaling regulates airway epithelial stem cells in adult murine submucosal glands. Stem Cells *34*, 2758–2771.

Lynch, T.J., Anderson, P.J., Rotti, P.G., Tyler, S.R., Crooke, A.K., Choi, S.H., Montoro, D.T., Silverman, C.L., Shahin, W., Zhao, R., et al. (2018). Submucosal gland myoepithelial cells are reserve stem cells that can regenerate mouse tracheal epithelium. Cell Stem Cell *22*, 653–667.e5.

McQualter, J.L., Yuen, K., Williams, B., and Bertoncello, I. (2010). Evidence of an epithelial stem/progenitor cell hierarchy in the adult mouse lung. Proc. Natl. Acad. Sci. U S A *107*, 1414–1419.

De Moerlooze, L., Spencer-Dene, B., Revest, J.M., Hajihosseini, M., Rosewell, I., and Dickson, C. (2000). An important role for the IIIb isoform of fibroblast growth factor receptor 2 (FGFR2) in mesenchymal-epithelial signalling during mouse organogenesis. Development *127*, 483–492.

Nakano, Y., Yang, I.V., Walts, A.D., Watson, A.M., Helling, B.A., Fletcher, A.A., Lara, A.R., Schwarz, M.I., Evans, C.M., and Schwartz, D.A. (2016). MUC5B promoter variant rs35705950 affects MUC5B expression in the distal airways in idiopathic pulmonary fibrosis. Am. J. Respir. Crit. Care Med. *193*, 464–466.

Ostedgaard, L.S., Moninger, T.O., McMenimen, J.D., Sawin, N.M., Parker, C.P., Thornell, I.M., Powers, L.S., Gansemer, N.D., Bouzek, D.C., Cook, D.P., et al. (2017). Gel-forming mucins form distinct morphologic structures in airways. Proc. Natl. Acad. Sci. U S A *114*, 6842–6847.

Plantier, L., Crestani, B., Wert, S.E., Dehoux, M., Zweytick, B., Guenther, A., and Whitsett, J.A. (2011). Ectopic respiratory epithelial cell differentiation in bronchiolised distal airspaces in idiopathic pulmonary fibrosis. Thorax *66*, 651–657.

Ray, S., Chiba, N., Yao, C., Guan, X., McConnell, A.M., Brockway, B., Que, L., McQualter, J.L., and Stripp, B.R. (2016). Rare SOX2+ airway progenitor cells generate KRT5+ cells that repopulate damaged alveolar parenchyma following influenza virus Infection. Stem Cell Reports *7*, 817–825.

Redente, E.F., Keith, R.C., Janssen, W., Henson, P.M., Ortiz, L.A., Downey, G.P., Bratton, D.L., and Riches, D.W. (2014). Tumor necrosis factor-alpha accelerates the resolution of established pulmonary fibrosis in mice by targeting profibrotic lung macrophages. Am. J. Respir. Cell Mol. Biol. *50*, 825–837.

Rock, J.R., Barkauskas, C.E., Cronce, M.J., Xue, Y., Harris, J.R., Liang, J., Noble, P.W., and Hogan, B.L. (2011). Multiple stromal populations contribute to pulmonary fibrosis without evidence for epithelial to mesenchymal transition. Proc. Natl. Acad. Sci. U S A *108*, E1475–E1483.

Roy, M.G., Rahmani, M., Hernandez, J.R., Alexander, S.N., Ehre, C., Ho, S.B., and Evans, C.M. (2011). Mucin production during pre- and post-natal mouse lung development. Am. J. Respir. Cell Mol. Biol. *44*, 755–760.

Roy, M.G., Livraghi-Butrico, A., Fletcher, A.A., McElwee, M.M., Evans, S.E., Boerner, R.M., Alexander, S.N., Bellinghausen, L.K., Song, A.S., Petrova, Y.M., et al. (2014). Muc5b is required for airway defence. Nature *505*, 412–416.

Seibold, M.A., Wise, A.L., Speer, M.C., Steele, M.P., Brown, K.K., Loyd, J.E., Fingerlin, T.E., Zhang, W., Gudmundsson, G., Groshong, S.D., et al. (2011). A common MUC5B promoter polymorphism and pulmonary fibrosis. N. Engl. J. Med. *364*, 1503–1512.

Seibold, M.A., Smith, R.W., Urbanek, C., Groshong, S.D., Cosgrove, G.P., Brown, K.K., Schwarz, M.I., Schwartz, D.A., and Reynolds, S.D. (2013). The idiopathic pulmonary fibrosis honeycomb cyst contains a mucocilary pseudostratified epithelium. PLoS One *8*, e58658.

Steele, M.P., and Schwartz, D.A. (2013). Molecular mechanisms in progressive idiopathic pulmonary fibrosis. Annu. Rev. Med. *64*, 265–276.

Tata, A., Kobayashi, Y., Chow, R.D., Tran, J., Desai, A., Massri, A.J., McCord, T.J., Gunn, M.D., and Tata, P.R. (2018). Myoepithelial cells of submucosal glands can function as reserve stem cells to regenerate airways after injury. Cell Stem Cell *22*, 668–683.e6.

Thannickal, V.J., Toews, G.B., White, E.S., Lynch, J.P., 3rd, and Martinez, F.J. (2004). Mechanisms of pulmonary fibrosis. Annu. Rev. Med. *55*, 395–417.

Urness, L.D., Paxton, C.N., Wang, X., Schoenwolf, G.C., and Mansour, S.L. (2010). FGF signaling regulates otic placode induction and refinement by controlling both ectodermal target genes and hindbrain Wnt8a. Dev. Biol. *340*, 595–604.

Vaughan, A.E., Brumwell, A.N., Xi, Y., Gotts, J.E., Brownfield, D.G., Treutlein, B., Tan, K., Tan, V., Liu, F.C., Looney, M.R., et al. (2015). Lineage-negative progenitors mobilize to regenerate lung epithelium after major injury. Nature *517*, 621–625.

Volckaert, T., and De Langhe, S. (2014). Lung epithelial stem cells and their niches: Fgf10 takes center stage. Fibrogenesis Tissue Repair *7*, 8.

Volckaert, T., Dill, E., Campbell, A., Tiozzo, C., Majka, S., Bellusci, S., and De Langhe, S.P. (2011). Parabronchial smooth muscle constitutes an airway epithelial stem cell niche in the mouse lung after injury. J. Clin. Invest. *121*, 4409–4419.

Volckaert, T., Campbell, A., Dill, E., Li, C., Minoo, P., and De Langhe, S. (2013). Localized Fgf10 expression is not required for lung branching morphogenesis but prevents differentiation of epithelial progenitors. Development *140*, 3731–3742.

Volckaert, T., Yuan, T., Chao, C.M., Bell, H., Sitaula, A., Szimmtenings, L., El Agha, E., Chanda, D., Majka, S., Bellusci, S., et al. (2017). Fgf10-Hippo epithelial-mesenchymal crosstalk maintains and recruits lung basal stem cells. Dev. Cell *43*, 48–59.e5.

Wendling, O., Bornert, J.M., Chambon, P., and Metzger, D. (2009). Efficient temporally-controlled targeted mutagenesis in smooth muscle cells of the adult mouse. Genesis *47*, 14–18.

Xi, Y., Kim, T., Brumwell, A.N., Driver, I.H., Wei, Y., Tan, V., Jackson, J.R., Xu, J., Lee, D.K., Gotts, J.E., et al. (2017). Local lung hypoxia determines epithelial fate decisions during alveolar regeneration. Nat. Cell Biol. *19*, 904–914.

Xie, T., Wang, Y., Deng, N., Huang, G., Taghavifar, F., Geng, Y., Liu, N., Kulur, V., Yao, C., Chen, P., et al. (2018). Single-cell deconvolution of fibroblast heterogeneity in mouse pulmonary fibrosis. Cell Rep. *22*, 3625–3640.

Xu, Y., Mizuno, T., Sridharan, A., Du, Y., Guo, M., Tang, J., Wikenheiser-Brokamp, K.A., Perl, A.T., Funari, V.A., Gokey, J.J., et al. (2016). Single-cell RNA sequencing identifies diverse roles of epithelial cells in idiopathic pulmonary fibrosis. JCI Insight *1*, e90558.

Yang, J., Wheeler, S.E., Velikoff, M., Kleaveland, K.R., LaFemina, M.J., Frank, J.A., Chapman, H.A., Christensen, P.J., and Kim, K.K. (2013). Activated alveolar epithelial cells initiate fibrosis through secretion of mesenchymal proteins. Am. J. Pathol. *183*, 1559–1570.

Yang, Y., Riccio, P., Schotsaert, M., Mori, M., Lu, J., Lee, D.K., Garcia-Sastre, A., Xu, J., and Cardoso, W.V. (2018). Spatial-temporal lineage restrictions of embryonic p63(+) progenitors establish distinct stem cell pools in adult airways. Dev. Cell *44*, 752–761.e4.

Zhang, Y., Noth, I., Garcia, J.G., and Kaminski, N. (2011). A variant in the promoter of MUC5B and idiopathic pulmonary fibrosis. N. Engl. J. Med. *364*, 1576–1577.

Zheng, D., Limmon, G.V., Yin, L., Leung, N.H., Yu, H., Chow, V.T., and Chen, J. (2012). Regeneration of alveolar type i and ii cells from scgb1a1-expressing cells following severe pulmonary damage induced by bleomycin and influenza. PLoS One *7*, e48451.

Zheng, D., Yin, L., and Chen, J. (2013). Evidence for Scgb1a1 cells in the generation of p63 cells in the damaged lung parenchyma. Am. J. Respir. Cell Mol. Biol. *50*, 595–604.

Zuo, W., Zhang, T., Wu, D.Z., Guan, S.P., Liew, A.A., Yamamoto, Y., Wang, X., Lim, S.J., Vincent, M., Lessard, M., et al. (2015). p63Krt5 distal airway stem cells are essential for lung regeneration. Nature *517*, 616–620.